Collapse of High Field Magnetophonon Resonance in GaAs-GaAlAs Heterojunctions

D. R. Leadley,[1] R. J. Nicholas,[1] J. Singleton,[1,4] W. Xu,[2,3] F.M. Peeters,[2] J. T. Devreese,[2] J. A. A. J. Perenboom,[4] L. van Bockstal,[5] F. Herlach,[5] J. J. Harris,[6] and C. T. Foxon[7]

[1]*Department of Physics, University of Oxford, Clarendon Laboratory, Parks Road, Oxford, OX1 3PU, United Kingdom*
[2]*Departement Natuurkunde, Universiteit Antwerpen (UIA), Universiteitsplein 1, B- 2610 Antwerpen, Belgium*
[3]*Department of Theoretical Physics, The Australian National University, Canberra, 0200, Australia*
[4]*University of Nijmegen, Toernooiveld 1, NL-6525 ED, Nijmegen, The Netherlands*
[5]*Katholieke Universiteit Leuven, Celestijnenlaan 2000, B-3001, Leuven, Belgium*
[6]*Department of Electronics and Electrical Engineering, University College London, London, United Kingdom*
[7]*Department of Physics, Nottingham University, Nottingham, United Kingdom*

(Received 11 April 1994)

Magnetophonon resonance is studied in the resistivity of high mobility GaAs-GaAlAs heterojunctions. In contrast to previous studies which show an exponentially damped series of oscillations, we find this only at low magnetic fields. At high fields the oscillation amplitude decreases, leading to collapse of the fundamental resonance. Fully self-consistent calculations, including *all* scattering processes, show that Landau level width oscillates in field and explain this unusual behavior.

PACS numbers: 73.40.Kp

Magnetophonon resonance (MPR) leads to a series of exponentially damped oscillations in the resistivity ρ_{xx} of semiconductors due to the resonant absorption and emission of longitudinal optic (LO) phonons. It has been used to extract information about the band structure of bulk and reduced dimensional semiconductors for the past three decades and has been reviewed several times [1– 3]. This paper is concerned with high mobility, low electron density, GaAs-GaAlAs heterojunctions where we find the MPR oscillations in the resistivity are qualitatively different from any previous reports. Most strikingly the oscillations at the highest magnetic fields B, expected to be the strongest features in ρ_{xx}, completely disappear. By including all the scattering mechanisms which affect the resistivity self-consistently, we can calculate the temperature and B dependence of ρ_{xx} and the density of states (DOS). These calculations reproduce the new experimental results extremely well and show for the first time that the Landau level (LL) broadening Γ oscillates with magnetic field at high temperature [4]. For LLs above the LO phonon energy the shape is dramatically changed by the resonant inelastic scattering.

The resonance in electron-optic phonon scattering (OPS) occurs whenever the LO phonon energy $\hbar\omega_{\mathrm{LO}}$ is equal to an integral multiple of the cyclotron energy:

$$\omega_{\mathrm{LO}} = N\omega_c = NeB/m^*, \qquad N = 1, 2, 3, \ldots. \tag{1}$$

Conservation of crystal momentum in 2D systems limits the optic phonon wave vector allowing the phonon to be regarded as monoenergetic, and so the MPR oscillations probe the electronic DOS at high temperature. Effective mass values m^* and deviations from the band edge value, due to nonparabolicity and polaron enhancement, have been obtained for a wide variety of materials from the fields of the resonances. Further information on the DOS and electron phonon coupling strength may be extracted by comparing the amplitude and line shape of the oscillations with a detailed theoretical model. MPR has usually been studied in ρ_{xx}, but oscillations have been seen in most transport coefficients as well as in optical absorption and cyclotron resonance [1–3,5].

Empirically the MPR oscillations in ρ_{xx} have been described by an exponentially damped cosine series,

$$\frac{\Delta\rho_{xx}}{\rho_{xx}} \propto \cos(2\pi\omega_{\mathrm{LO}}/\omega_c)\exp(-\gamma\omega_{\mathrm{LO}}/\omega_c). \tag{2}$$

This formula was first suggested from experiments on bulk GaAs [6] where the damping factor γ was found to be constant in magnetic field but to vary with temperature and sample mobility. By considering short range scattering, Eq. (2) was also found as the first term in a harmonic expansion for the conductivity [7], which relates the empirical γ to the LL width by $\gamma = 2\pi\Gamma/\hbar\omega_{\mathrm{LO}}$. *All* previous experimental MPR studies on materials ranging from silicon to II-VI alloys could be described by this exponentially damped series, although quantitative agreement was often difficult, especially when γ varied with B rendering the form of Eq. (2) inappropriate. However, in high mobility GaAs-GaAlAs heterojunctions we find a very different behavior, particularly in samples with a wide undoped GaAlAs spacer layer.

The magnetoresistance has been measured in a large number of GaAs-GaAlAs heterojunctions in pulsed fields up to 36 T at KU Leuven and steady fields to 30 T using the Nijmegen hybrid magnet. The samples were grown by molecular beam epitaxy at Philips Research Laboratories to a standard design [8] with the properties shown in Table I.

The two extreme types of behavior observed in these samples are illustrated in Fig. 1, which shows ρ_{xx} for samples with spacer layer widths L_z of 400 Å and 3200 Å.

0031-9007/94/73(4)/589(4)$06.00

TABLE I. Sample parameters: n_e is measured at 4 K in the dark and μ_0 is the zero-temperature impurity limited mobility. L_z is the width of the undoped GaAlAs spacer layer.

Sample	L_z(Å)	$n_e(10^{15}$ m$^{-2})$	μ_0(m^2/V s)
G647	3200	0.15	30
G641	1600	0.25	170
G137	1600	0.31	33
G141	800	0.9	102
G156	800	1.0	76
G148	400	2.0	96
G590	100	3.2	16

To emphasize the oscillations the monotonic background resistance has been subtracted and the result expressed as a fraction of the zero-field resistance ρ_0. The thinner spacer layer sample G148 shows fairly conventional MPR, exhibiting a damped cosine series. However, the results are quite different for the wider spacer layer sample G647, which also has a lower electron density n_e. The oscillations at low magnetic field are well resolved, larger and less damped than those for sample G148, but the amplitude is largest for the $N = 4$ resonance at 5.5 T while the fundamental $N = 1$ resonance has become very weak. This behavior can clearly not be explained by Eq. (2). Even for sample G148 Eq. (2) does not give quantitative agreement, since the higher field peaks have not increased as much as expected [9].

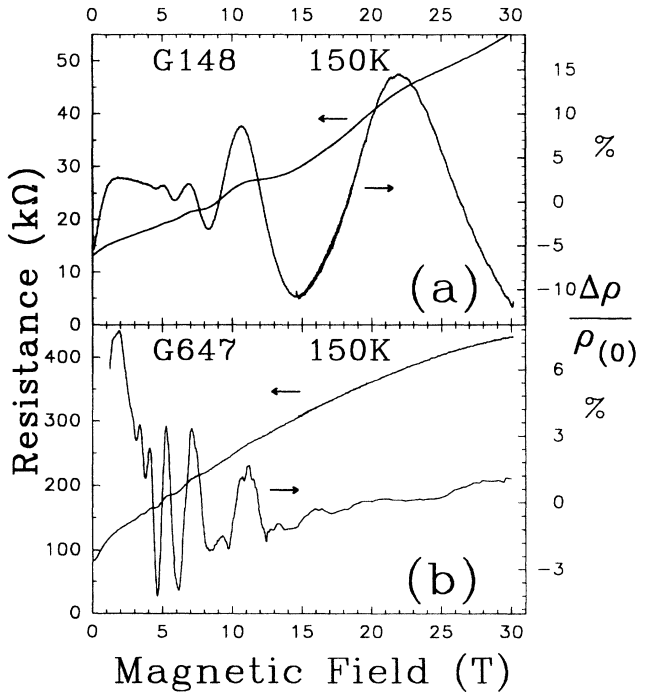

FIG. 1. (a) The magnetoresistance of a narrow spacer layer sample G148 showing conventional MPR (left scale). The oscillations are enhanced by subtracting the background and dividing by ρ_0 (right scale). (b) The same for a wide spacer layer sample G647 showing conventional MPR at low field but collapse of the $N = 1$ resonance at high field.

The amplitude of the four highest field resonances are shown in Fig. 2 for each sample in Table I. For low values of L_z the amplitude increases at higher B (smaller N) while for samples with a large L_z the reverse is true. Thus for each harmonic there is a maximum amplitude, occurring at larger L_z for higher N. Temperature is also important: for sample G647 the $N = 2$ resonance which is quite strong at 180 K has virtually disappeared by 120 K while the $N = 3$ peak also weakens markedly relative to the $N = 4$ peak as the temperature is reduced.

All the samples follow the same general behavior: (i) At low magnetic fields the oscillations increase in amplitude with field as described by Eq. (2). (ii) At high fields the amplitudes decrease quite rapidly with increasing field and even disappear completely. (iii) The crossover moves to lower field (a) at lower temperatures and (b) in samples with wider spacer layers (lower n_e).

We will now explain the anomalous experimental results by calculating ρ_{xx} with all the scattering processes included self-consistently. The full self-consistency is essential in calculating both the density of states and the resistivity, since each scattering mechanism is significantly affected by (and significantly affects) the DOS.

Previous MPR calculations used a short range scattering approximation where each LL is treated as Gaussian or semielliptic with the same width $\Gamma(B) = \sqrt{2\hbar\omega_c\Gamma_0/\pi}$ [10,11], i.e., $\Gamma(B) \propto \sqrt{B}$. Sample dependent effects were parametrized by Γ_0, which is related to the zero-field mobility μ_0. In this approach ρ_{xx} can only *increase* at the MPR condition Eq. (1) due to the additional scattering. This inevitably leads to larger oscillations at higher B where the number of states at the center of the LLs is

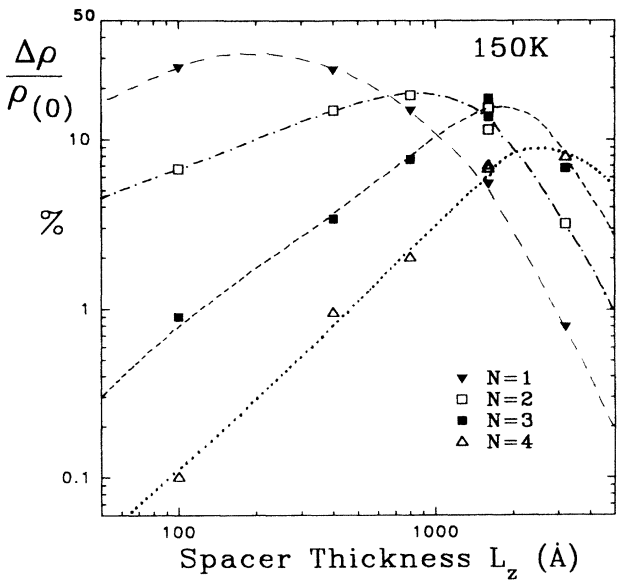

FIG. 2. Amplitude of MPR peaks for samples of different spacer layer thicknesses. The lines are guides to the eye.

greater. Thus the decrease in oscillation amplitude at high field, seen in Fig. 1(b), could not be explained.

Our calculations are based on a Green's function approach to the momentum balance equation. Details may be found in Ref. [12] where we calculated ρ_{xx} as a function of temperature for fixed magnetic fields. We include elastic scattering from impurities [I] and acoustic phonons [A], and inelastic LO phonon scattering [O]. For the calculations reported here we have removed some of the simplifying assumptions of Ref. [12] . The impurities are now treated more realistically as Coulomb potentials and remote ionized impurities are included explicitly, with their density taken from the measured n_e. The background impurity density is evaluated from fitting μ_0, giving values of 2.3×10^{14} cm^{-3} and 4.7×10^{14} cm^{-3} for samples G647 and G148. Piezoelectric and deformation potential coupling to acoustic phonons are both now included.

We write the resistivity as a product of scattering matrix elements $\mathcal{R}_{M'M}$ and an integration over the joint density of initial and final states $\mathcal{F}_{M'M}$, subject to energy conservation for *elastic* or *inelastic* scattering, summed over initial M and final M' LLs:

$$\rho_{xx} = \sum_{M'M} (\mathcal{R}^I_{M'M} + \mathcal{R}^A_{M'M})\,\mathcal{F}^{\rm el}_{M'M} + \mathcal{R}^O_{M'M}\mathcal{F}^{\rm in}_{M'M}, \quad (3)$$

$$\mathcal{F}^{\rm el}_{M'M} = \int_{-\infty}^{\infty} dE \frac{\partial f(E)}{\partial E} {\rm Im}G_{M'}(E){\rm Im}G_M(E),$$

$$\mathcal{F}^{\rm in}_{M'M} = \int_{-\infty}^{\infty} dE[f(E) - f(E + \hbar\omega_{\rm LO})] \quad (4)$$

$$\times\, {\rm Im}G_{M'}(E + \hbar\omega_{\rm LO})\,{\rm Im}G_M(E),$$

where ${\rm Im}G_M(E)$ is the imaginary part of the Green's function, proportional to the DOS for the Mth LL, and $G_M(E) = [E - E_M - \Sigma_M(E)]^{-1}$, centered at energy $E_M = (M + 1/2)\hbar\omega_c$ with a self-energy of

$$\Sigma_M(E) = \sum_{M'} \Big\{ (\mathcal{W}^{\rm I}_{M'M} + \mathcal{W}^{\rm A}_{M'M})\,G_{M'}(E) + \mathcal{W}^{\rm O}_{M'M}[N_0 + f(E - E_{M'})] \times G_{M'}(E + \hbar\omega_{\rm LO}) + \mathcal{W}^{\rm O}_{M'M}[N_0 + 1 - f(E - E_{M'})] \times G_{M'}(E - \hbar\omega_{\rm LO}) \Big\}. \quad (5)$$

$f(E)$ is the Fermi-Dirac electron distribution function and N_0 is the LO phonon occupation number. The $\mathcal{W}^i_{M'M}$ are also scattering matrix elements, closely related to $\mathcal{R}^i_{M'M}$ in their dependence on temperature, magnetic field, and sample parameters. However, while the $\mathcal{W}$ terms weight all scattering events equally, the $\mathcal{R}$ terms also account for the momentum transferred. As most scattering events are isotropic the ratio $\mathcal{R}^i/\mathcal{W}^i$ is essentially the same for all scattering mechanisms. The exception is the small angled scattering from remote ionized impurities which makes $\mathcal{R}^{\rm I}$ particularly small, with $\mathcal{R}^{\rm I}/\mathcal{W}^{\rm I}$ determined by the spacer layer thickness provided the background impurity scattering is not too large. Exact forms of these matrix elements are in Ref. [12], but note that (a) elastic terms increase faster with B than inelastic terms, and (b) OPS terms increase rapidly with temperature.

Equations (3)–(5) must be solved self consistently for G_M to calculate ρ_{xx} and the DOS. In Ref. [12], we calculated ρ_{xx} using semielliptic LLs, each with a width Γ_M evaluated at the center of the level for every field and temperature. Now we retain the full energy dependent Green's functions throughout the calculation. For LLs with $E_M < \hbar\omega_{\rm LO}$ the DOS is still essentially semielliptic with a width that shows striking increases at the MPR condition due to the additional scattering. This produces a Γ_M that oscillates in field and is different for each LL. For higher LLs where electrons can both emit and absorb LO phonons there is a dramatic change in the shape of the DOS at resonance. A reduction in DOS at the center of the level is accompanied by the appearance of wings at the edges, where the resonance condition is no longer satisfied [13].

Using this self-consistent DOS we find two sources of oscillations in Eq. (3) as shown in Fig. 3 where we separate the elastic and inelastic parts. At the MPR condition $\mathcal{F}^{\rm in}$ is enhanced, giving the expected *increase* in resistivity at resonance. However, terms in the Green's functions containing $\mathcal{W}^{\rm O}$ also increase and broaden the LLs, which *decreases* both $\mathcal{F}^{\rm el}$ and $\mathcal{F}^{\rm in}$. Thus the amplitude of the MPR oscillations in ρ_{xx} depends on competition between the elastic and inelastic terms in both Eq. (3) and (5).

Let us now examine the effect of changing the relative sizes of the matrix elements. On increasing the inelastic terms relative to the elastic terms, for instance, by raising the temperature at fixed B, the final (inelastic) term in Eq. (3) will start to dominate the resistivity as $\mathcal{R}^{\rm I}$ is small, while the DOS is still largely determined by the elastic terms because $\mathcal{W}^{\rm I}$ is not small. Thus the MPR amplitude will increase. On further increasing the

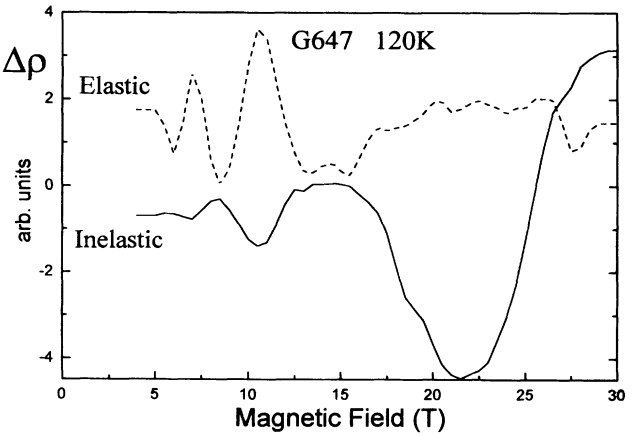

FIG. 3. The calculated oscillatory parts of ρ_{xx} showing positive and negative contributions to the MPR from inelastic and elastic scattering. (Note that the total value of ρ_{xx} is not simply the sum of these two contributions due to the self-consistency.)

inelastic terms it will decrease again as $\mathcal{W}^0$ starts to dominate $\mathcal{W}^1$ in Eq. (5). Hence the MPR amplitude has a maximum as a function of temperature, as observed at ~ 150 K [3]. The maximum we see as a function of field can also be explained by considering the crossover to domination by elastic terms as B is increased. With no inelastic scattering both Eqs. (3) and (5) are dominated by the elastic processes and there will clearly be no MPR. In fact if any one type of scattering dominates the MPR will be weak, as the oscillatory parts approximately cancel and the conductivity remains constant. (A similar effect occurs for low temperature Shubnikov–de Haas oscillations, where the conductivity maxima values can become independent of scattering rate [14].)

Figure 4 shows how calculations reproduce the data of Fig. 1. Note that both oscillatory and background parts of ρ_{xx} are calculated directly and give good agreement over the whole field range using only sample parameters determined at $B = 0$. By contrast, earlier approaches calculated only the oscillatory part [7,11] or gave a constant background in the field region of interest [15,10]. Calculations that are not fully self-consistent also lead to very substantial overestimates of the oscillations.

The general behavior described in the experiments earlier can now be explained: (i) At low magnetic fields and high temperatures LO phonon scattering has a much greater effect than elastic scattering on ρ_{xx}, so oscillations in the OPS rate $\mathcal{F}^{\text{in}}$ lead directly to MPR oscillations in ρ_{xx}. (ii) At high magnetic fields the LLs are very sharp and ρ_{xx} is essentially determined by elastic scattering and the number of states at the center of each level.

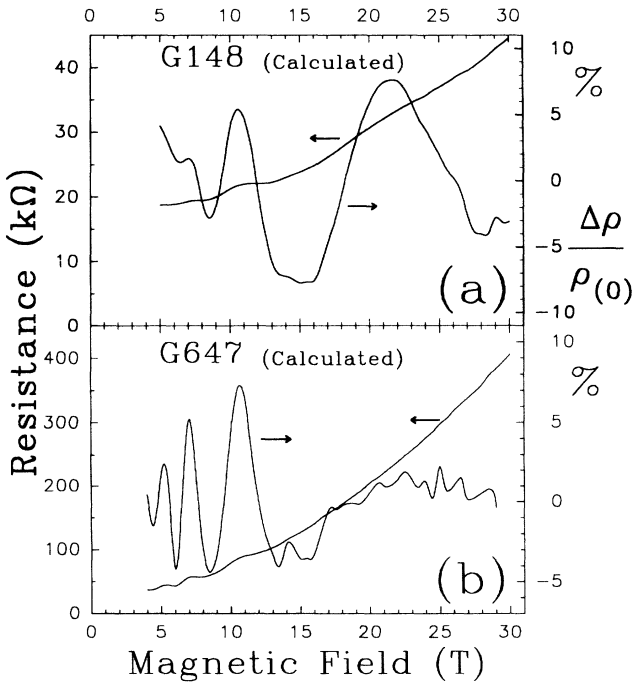

FIG. 4. The calculated ρ_{xx} for the parameters of the samples in Fig. 1.

The reduction in DOS at resonance dramatically reduces the overall scattering rate, compensating for the increase in OPS and resulting in smaller or vanishing MPR oscillations. (iii) (a) By reducing LO phonon scattering at lower temperatures type (ii) behavior will be seen at lower fields. (b) At a fixed temperature and a magnetic field where strong MPR is expected, the resonances are most likely to disappear when the oscillations in LL width as a function of B are large. This occurs when the impurity scattering is small, which is true for samples with a low background impurity density and a wide spacer layer. By comparison in 3D or low mobility samples there will always be a considerable number of states between LLs and so resonances in $\mathcal{F}^{\text{in}}$ will dominate the oscillating level width, giving the exponentially damped series.

In conclusion, magnetophonon resonance in the resistance of very high purity samples is substantially different from that seen previously. Instead of an exponential increase with magnetic field, there is a strong reduction of amplitude at high magnetic fields and in certain situations the $N = 1$ resonance almost disappears. Increased inelastic scattering at resonance reduces the density of states and so to calculate ρ_{xx} all scattering mechanisms must be considered self-consistently. By such calculations we are able to reproduce the experimental data.

We acknowledge support from the British-Flemish Academic Research Collaboration Programme; the Rutherford Appleton Laboratory (DRL) and the Belgian National Science Foundation (FMP).

[1] R. J. Nicholas, Prog. Quantum Electron. **10**, 1 (1985).
[2] R. L. Peterson, in *Semiconductors and Semimetals*, edited by R. K. Willardson and A. C. Beer (Academic, New York, 1975), Vol. 10, p. 221.
[3] R. J. Nicholas, in *Landau Level Spectroscopy*, edited by G. Landwehr and E. I. Rashba (Elsevier, Amsterdam, 1991), p. 777.
[4] This oscillatory Γ at high temperatures and filling factors $\nu \ll 1$ arises from changes in inelastic scattering rate with B and should not be confused with the effects of oscillatory screening seen at low temperature and $\nu > 1$.
[5] D. J. Barnes *et al.*, Phys. Rev. Lett. **66**, 794 (1991).
[6] R. Stradling and R. Wood, J. Phys. C **1**, 1711 (1968).
[7] J. R. Barker, J. Phys. C **5**, 1657 (1972).
[8] C. T. Foxon, J. J. Harris, D. Hilton, J. Hewett, and C. Roberts, Semicond. Sci. Technol. **4**, 582 (1989).
[9] D. R. Leadley *et al.*, in *High Magnetic Fields in Semiconductor Physics III,* Springer Series in Solid State Sciences Vol. 101 (Springer, Berlin, 1992), p. 623.
[10] R. Lassnig and W. Zawadzki, J. Phys. C **16**, 5435 (1983).
[11] P. Warmenbol, F. M. Peeters, and J. T. Devreese, Phys. Rev. B **37**, 4694 (1988).
[12] D. R. Leadley *et al.*, Physica (Amsterdam) **184B**, 197 (1993); Phys. Rev. B **48**, 5457 (1993).
[13] W. Xu *et al.*, in Proceedings of the ICPS-22, Vancouver, 1994 (to be published).
[14] T. Ando, J. Phys. Soc. Jpn. **37**, 1233 (1974).
[15] N. Mori *et al.*, Phys. Rev. B **38**, 7622 (1988).